JETIR.ORG ISSN: 2349-5162 | ESTD Year : 2014 | Monthly Issue
JOURNAL OF EMERGING TECHNOLOGIES AND INNOVATIVE RESEARCH (JETIR)
An International Scholarly Open Access, Peer-reviewed, Refereed Journal

Design and Testing of Experimental Langmuir Turbulence Facilities

[1]Gulshan kumar,[2]Omprakash S.Thakare ,[3]Ajay Kumar Gupta

[1]Mtech Scholar,[2]Assistant Professor,[3]Professor
[1]MTech (Production Engineering),
[1]Shri Rawatpura Sarkar University, Raipur(c.g.),India

Abstract : *Langmuir Circulation is a common phenomenon driven by wind in oceans and lakes and was first studied by Langmuir in 1927. According to various ocean observations, this kind of phenomenon plays an important role in many phenomena such as the aggregation of bubbles, the distribution of plankton as well as the mixing of spilled oil and sediment in the ocean. To study this, an experimental facility has been developed in the lab which creates a small scale version of Langmuir Circulation. This thesis is about the design and testing of this tank and surrounding aluminum frame, as well as the design and construction of the illumination equipment (the Green Lantern 2.0) needed for Particle Image Velocimetry measurements within the tank. ANSYS will be used to show whether the tank is structurally strong enough to support the fluid. An enhancement is found that prevents a frontward bend of tank wall, which is analyzed by ANSYS to find an optimized construction to minimize tank deformation. Then, the Light-Emitting Diode (LED) and collimating lens selection for the Green Lantern 2.0 will also be shown in this paper. Besides, this thesis also presents preliminary flow measurement data acquired using the illumination equipment (the Green Lantern).*

I. INTRODUCTION

Langmuir turbulence (LT) is believed to be one of the leading order causes of turbulent mixing in the upper ocean, which is important for momentum and heat exchange across the air–sea interface and between the mixed layer and the thermo cline. Both observational studies(D'Asaro,2001,2014) and large-eddy simulation (LES) investigations(Li et al.,1995;Kukulka et al.,2009,2010;Skylingstad and Denbo,1995;McWilliams et al.,1997;Hamlington et al.,2014) have shown enhanced vertical mixing within the ocean surface boundary layer in the presence of LT through the enhanced vertical turbulent velocity variance.

The formation of Langmuir circulation can be briefly described like this: wind blows across the sea surface, drags water in the wind direction, and creates shear force on the water surface. Stokes drift which is induced by the surface waves interacts with the shear caused by wind and finally generates Langmuir circulation. At the junction of two vortices, there will be two cases: one is that two vortices combine to make the water flow up (i.e. upwelling), the other is that they combine to make the water flow down (i.e. down welling). For the second case, if particles in the water (e.g. Sargasso, oil droplets) are buoyant and can overcome the downward force caused by the fluid, then they will accumulate in the center of the two vortices in long windrows . The axis of the cells of Langmuir circulation has an angle of up to 20° to the right of the direction of the wind and the distance between cells can vary from 1 m to 300 m.

As researchers have studied Langmuir Circulation, its importance has become more and more evident. Because of the difficulty of studying Langmuir Circulation in the field, we have designed and built an experimental facility that creates a two dimensional "cartoon" of Langmuir Circulation in an acrylic tank in the laboratory. The focus of this thesis is on the design, testing, and subsequent modification of this experimental facility for future experiments examining the interaction of buoyant oil droplets and heavy sediment particles in Langmuir Circulation.

II. PREVALENT AND USE

Langmuir turbulence could have an important impact on our understanding of climate. In particular, Langmuir turbulence could affect the global ocean's sea surface temperature as the deeply penetrating Langmuir jets modify the depth of the ocean mixed layer.

III. LITERATURE REVIEW

1. McWilliams et al., 2014, Reichl et al., 2016b have shown the importance of including the Lagrangian shear in the parameterization of the turbulent momentum fluxes with LT. This is not considered here. The Lagrangian shear primarily affects the parameterization of the turbulent momentum flux in two ways. First by better aligning with the direction of the turbulent stress than when only using the Eulerian shear. This is however not an issue for us as KPP always imposes a current shear in the direction of the turbulent stress. The second effect is that the down-gradient mixing associated with Stokes drift shear will change the near surface Eulerian current, which may partially counter the Stokes advection term.

2. Takaya et al. (2010) (hereafter Tk10) proposed a refinement of a prognostic skin SST model by accounting for Langmuir turbulence mixing under stable conditions using a velocity scale by Grant and Belcher (2009). Although they did not test it in KPP, they followed the MS00 approach and proposed the scaling by Grant and Belcher (2009) as an LT enhancement

factor applied to the eddy diffusivity in their SST model in such way that it neglects the LT effects under large values of La_t. They have shown it to be successful in enhancing ocean mixing and reducing the diurnal variability of SST under wave's presence.

3. Van Roekel et al. (2012) (hereafter VR12), using a broadband empirical wave spectrum, introduced Langmuir mixing parameterization accounting for the misalignment between wind and wave directions, which is also based on a surface layer-averaged Langmuir number. Here, we use their adjusted enhancement factor for the conditions where wind and waves are aligned (Li et al., 2016). In addition, we adopt the LT enhancement of the boundary layer entrainment by modifying the bulk Richardson number with a Stokes drift term (Li et al., 2016).

4. Li and Fox-Kemper (2017) (hereafter LF17) investigated the LT effects on the entrainment buoyancy flux in the ocean surface boundary layer using LES with various combinations of wind, waves and (destabilizing) surface buoyancy flux. It is found that the entrainment is enhanced substantially under weakly convective conditions, while the effects are moderate under strongly convective turbulence. They therefore proposed an LT enhancement estimate of the scaling of the entrainment buoyancy flux at the base of the boundary layer, and derived a new expression for the unresolved turbulence shear velocity in the KPP scheme. Combined with a La_{ss}-based enhancement factor from Van Roekel et al. (2012), they have shown that this new modification has improved the MLD in the southern ocean in their Community Earth System Model (CESM) model simulations.

5. Large eddy simulation (LES) studies of the Langmuir circulation using the vortex force have shown considerable enhancement of the turbulent kinetic energy (TKE) in the surface boundary layer (e.g Skyllingstad and Denbo, 1995, McWilliams et al., 1997, Sullivan et al., 2007, McWilliams and Fox-Kemper, 2013). In an investigation to quantify the impact, D'Asaro et al. (2014) found an average increase of 15–20 % in MLD at high latitudes, as well as enhancement of the vertical turbulent kinetic energy (VKE) within the mixed layer by approximately a factor of two. Using LES solutions of the wave-averaged equations in a weakly convective, wind driven surface boundary layer.

6. McWilliams et al., 2014, Reichl et al., 2016b have shown the importance of including the Lagrangian shear in the parameterization of the turbulent momentum fluxes with LT. This is not considered here. The Lagrangian shear primarily affects the parameterization of the turbulent momentum flux in two ways. First by better aligning with the direction of the turbulent stress than when only using the Eulerian shear. This is however not an issue for us as KPP always imposes a current shear in the direction of the turbulent stress. The second effect is that the down-gradient mixing associated with Stokes drift shear will change the near surface Eulerian current, which may partially counter the Stokes advection term.

IV. RESEARCH METHODOLOGY

4.1 Tank Simulation:

As previous chapter mentioned, Langmuir Circulation consists of pairs of counter-rotating vortices, the experimental facilities (shown in Figure 3.1), which are used to simulate one of this pair of flow, consist of an acrylic tank (the object of the simulation in this chapter, shown in Figure3.2), motors, and conveyor belts. The water in the tank is driven by the conveyor belts on both sides of the tank to create a pair of counter-rotating vortices. Then, a high speed camera is used tocapture the flow in front of the tank.

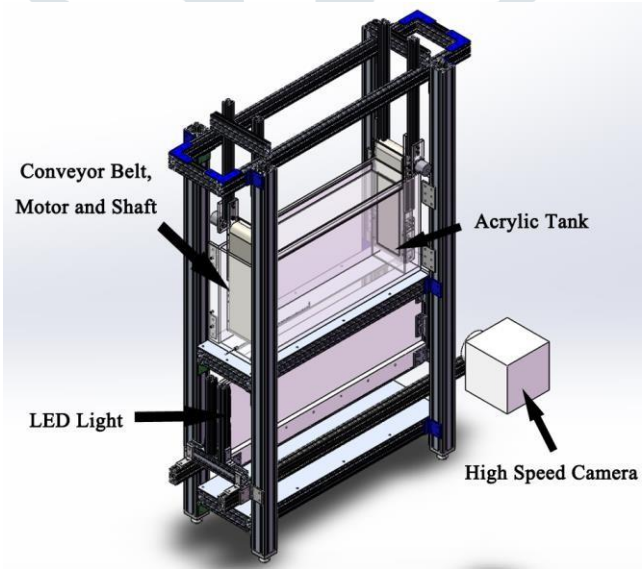

Figure 4.1 CAD Drawing of Langmuir Circulation Experimental Facility

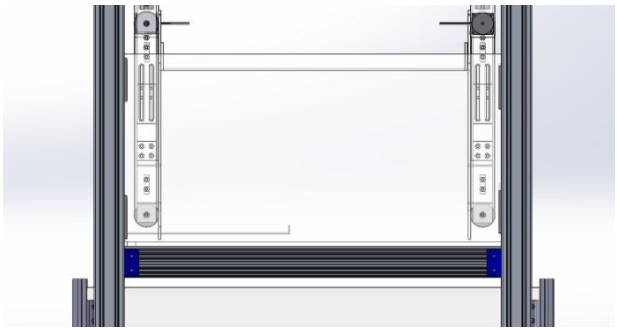

Figure4. 2 Front View of Langmuir Circulation Experimental Facility

However, it is observed that, when filled with water, the tank walls deform (up to 2 cm as will be shown in the following paragraphs). This may cause two problems: one is that the tank wall could break because of either the large deformation or the fatigue failure caused by multiple cycles of filling and draining it. The other concern is that since the high speed camera captures images through the tank wall, the wall deformation could distort the images.
Hence, in this chapter, ANSYS software will be used to show the performance of the acrylic tank. By using the Static Structural module, this software will determine how the tank will be in the real world from the aspects of deformation, equivalent stress and safety factor when the tank is 25%, 50%, 75%, and full of water. Then another simulation in which a brace is added across the opening of the tank is done to show the structural stability and reduction in deformation of the tank.

4.2 Model Geometry:

Two simulation models are tested: one is the tank alone, the other is the tank held with an aluminum clamp on the top in order to decrease the tank wall deformation. The original tank is modeled as a rectangular box, of which the length is 100 cm, the height is 50 cm, the width is 20 cm, and the wall thickness is 1.2 cm. In order to set the amount of water within the tank, the tank is divided vertically into 4 parts by 3 enclosed lines. The vertical distance between those enclosedlines is 12.5 cm. The configurations and the final model are shown in Figure 3 and Table 1.

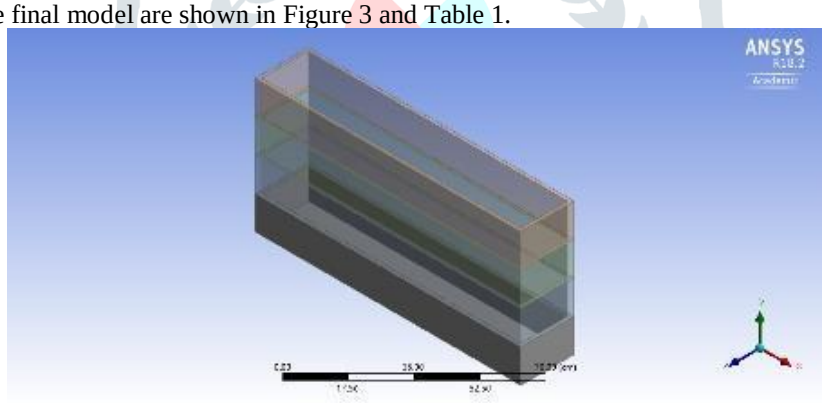

Figure 4.3 Original Tank Model

Table 4.1 Parameters of Original Tank

Property	Value (cm)
Tank Length	100
Tank Width	20
Tank Height	50
Tank Wall Thickness	1.2

Since initial experiments showed a large amount of tank wall deformation when the tank wasfilled, the need for a brace or clamp at the tank surface was apparent. Three different aluminum brace designs were generated and tested in ANSYS. Each brace consisted of a pair of extruded aluminum rails (80/20 Inc.) laying along the top of the tank walls. These rails are joined across the

tank by a pair of short extruded aluminum rails (80/20 Inc.) positioned at different distances from each other. The position for these rails which minimizes deformation and stress is found in this paper by changing the short beam location.

4.3 Original Tank Boundary Conditions:

For Static Structural boundary conditions, the material is set as an acrylic sheet first. There is only one part, so no connections need to be set. For mesh statistics, coarse quality is chosen, resulting in 24821 nodes and 4589 elements, as Figure 3.7 shows. For the fixed support option, the outer bottom of tank is chosen; hydrostatic pressure is used to simulate the real water pressure. Figure 3.8 shows the geometry of this case, the inner side faces of the tank are selected to set the hydrostatic pressure. Fluid density is selected to match the seawater in the Gulf of Mexico (e.g. 1027 kg/m^3)

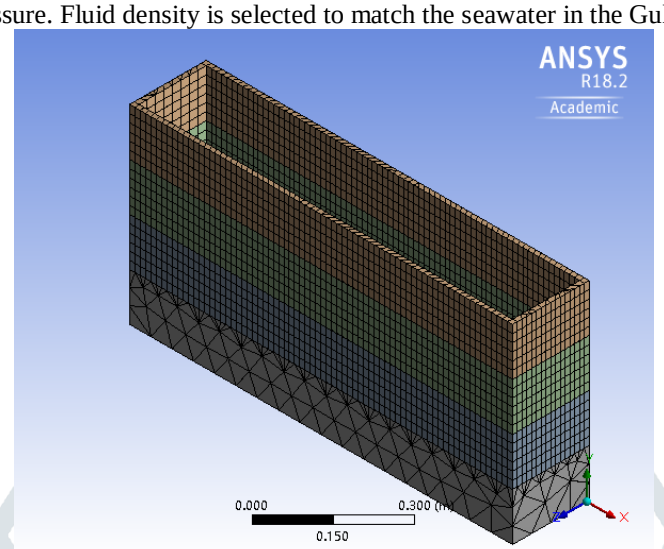

Figure 4.4 Original Tank Mesh

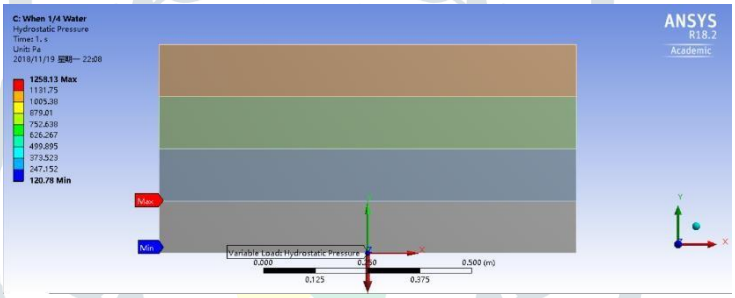

Figure 4.5 Hydrostatic Pressure for 1/4 Water

4.4 Boundary Conditions for the Improved Tank:

Four aluminum beams are added on the top of the tank, so the material is set to aluminum alloy for the beams. There are two parts, the tank and the brace, so a connection set is needed, as shown in Figure 3.9. The connection type is set to rough, so that there is friction between tank and clamp. A coarse mesh is used in this setting (there are 27665 nodes and 5005 elements), and the mesh is shown in Figure 3.10. The static structural settings are similar to the original tank case. The water is full in this case.

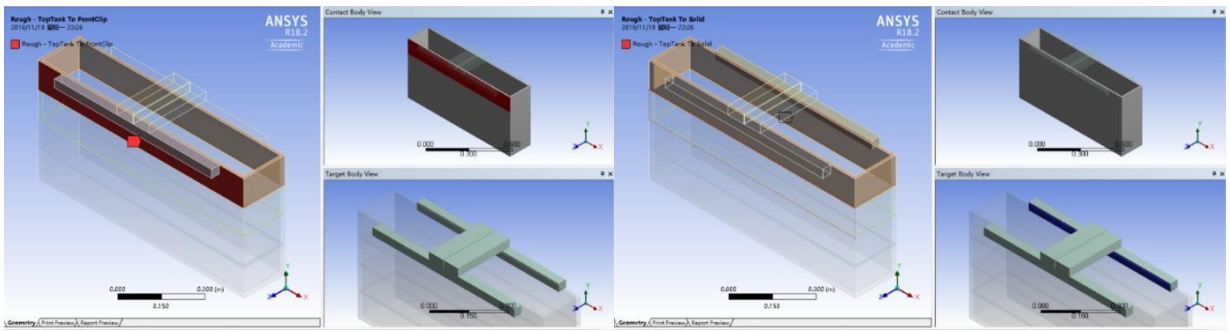

Figure 4.6 Connection Setting. (a. connection between front long beam and front wall of tank; b.connection between back long beam and back wall of tank)

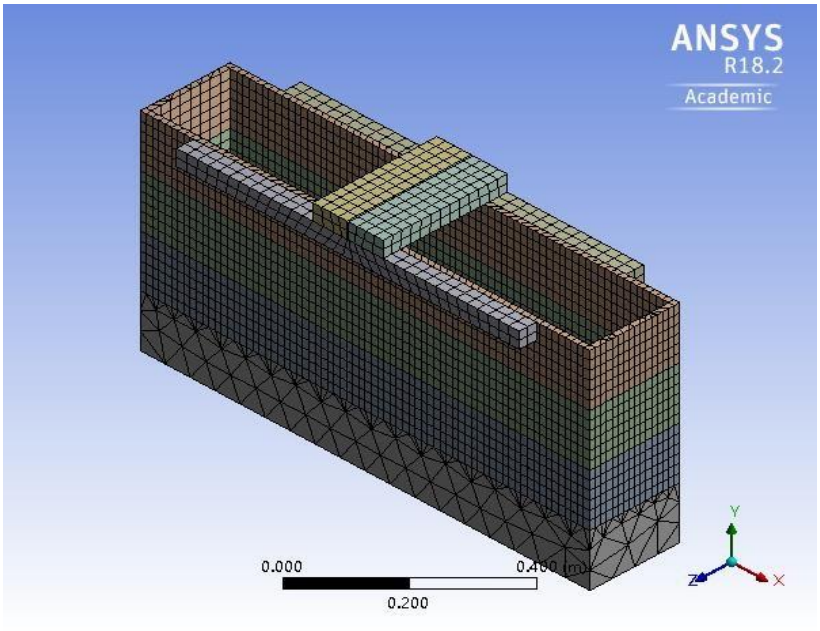

Figure 4.7 Improved Tank Mesh

V. EXPERIMENTAL SERTUP:

Generally, the experiment includes the following facilities:

(1) Acrylic tank: the reservoir for the water and tracers, the dimension is 1 m long × 0.2 m wide × 0.5 m deep.
(2) Conveyor belts, shafts and motors: used to force the fluid motion, the motors can provide multiple rotation speeds and run in clockwise and anti-clockwise directions.
(3) Tracer: because of the transparency of water, tracer is needed in this experiment for the flow to be captured by camera.
(4) High speed camera: used to get images for analysis after the experiment.
(5) High power LED light: use to provide enough brightness for the camera to capture the image.

The high speed camera is placed in the center of the front wall of the tank. The distance between the front wall of the tank and the lens of the camera is 1.58 m.

The main purpose of this experiment is to see the velocity field of the water in the tank at different speeds and rotation directions of the conveyor belt. The experiment can be divided into the following steps:

(1) Add tracer into the water to make the flow of water visible.
(2) Make the high speed camera focus on the light sheet.
(3) Put a calibration plate into the water in order to know the relation between the distance in the real world and in the image.
(4) Input the parameters to control the motor in order to drive the water flow.
(5) Stir the water in order to refloat the tracers and make the water flow random.
(6) Start the conveyor belts to drive the motion of the fluid.
(7) Wait until the water flow becomes stable.
(8) Capture an image sequence.
(9) Redo step (4) with different parameters till finish the image data collection.
(10) Calibrate the raw images captured in step (7) with PIV software.

(11) Analyze the calibrated images with PIV software.

For the parameters in step (4), the original motor step size is 1.8 degree. The resolution of the motor is set to 4, which means one original step is divided into 4 small steps. So, one step is 0.45 degree. 700 steps/s, 1400 steps/s, 2100 steps/s, 2800 steps/s and 3500 steps/s are used in this experiment and the circumference of the shaft is 6.35 cm, so the input velocities of the conveyor belts are 17.46 cm/s, 34.92 cm/s, 52.38 cm/s, 69.84 cm/s and 87.30 cm/s respectively. All PIV measurements and analysis were conducted in conjunction with Dr. Carlowen Smith.

Results and Conclusion

The time mean velocities for 700-3500 steps/s of both upwelling and down welling direction. It can be concluded that overall, the experimental setup can successfully create two counter-rotating vortices at different speeds and directions.

However, there are some differences between different experimental parameters. In the down welling flow, the vortices happen closer to the top of the tank. The vortices happen among the top 1/2 of the total water and the right vortex becomes large and less coherent as the speed of the fluid increases. Also, the area of convergence moves to the left as the speed is increased.

For the upwelling flow, the converging area nearly does not change with the speed of the fluid, it always happens at x ≈ 38cm. The location and size of the vortices, which occupies 3/5 to4/5 of the tank, are nearly constant. With the comparison of these images, it can be concluded that the vortices are most clear and distribute most evenly at the lowest speed and upwelling flow.

Figure 5.1 the mean fluid speed vs. the speed of the conveyor belts. The mean fluid speed generally increases as the conveyor belt speed increases. However, when the speed of the conveyor belt is at the maximum, which is 3500 steps/s, the mean velocity of the water drops down, this may be caused by the failure of the motor. When the motor tries to get 3500 steps/s, the force is too much to sustain at that rate of steps, then the actual speed of conveyor belt goes down, consequently causing the mean velocity of the water drops down.

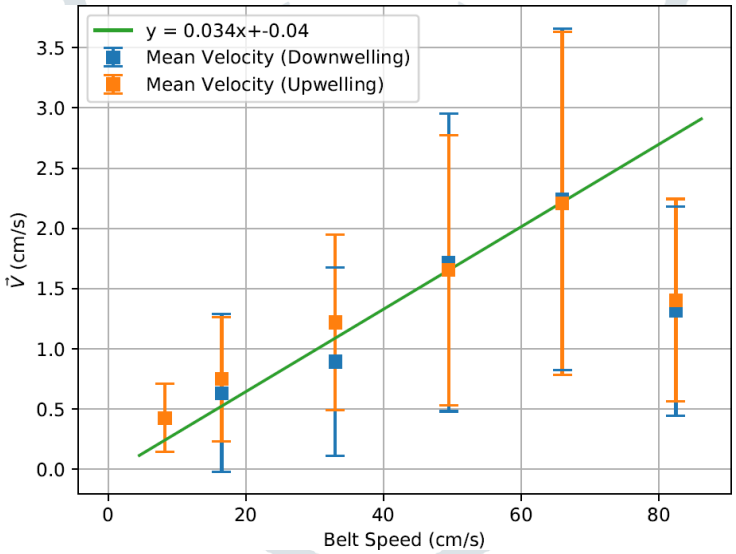

Figure 5.1 Mean Velocity of Water Vs Speed of Conveyor Belt

REFERENCES

[1] Bainbridge, R. (1957). The size, shape and density of marine phytoplankton concentrations. Biological Reviews, 32(1), 91-115.

[2] Langmuir, I. (1938). Surface motion of water induced by wind. Science, 87(2250), 119-123.

[3] Smith, J. A. (1992). Observed growth of Langmuir circulation. Journal of Geophysical Research: Oceans, 97(C4), 5651-5664.

[4] Thorpe, S. A. (2004). Langmuir circulation. Annu. Rev. Fluid Mech., 36, 55-79.

[5] Weller, R. A., & Price, J. F. (1988). Langmuir circulation within the oceanic mixed layer. Deep Sea Research Part A. Oceanographic Research Papers, 35(5), 711-747.

[6] Weller, R. A., Dean, J. P., Price, J. F., Francis, E. A., Marra, J., & Boardman, D. C. (1985). Three-dimensional flow in the upper ocean. Science, 227(4694), 1552-1556.

[7] Smith, J., Pinkel, R., & Weller, R. A. (1987). Velocity structure in the mixed layer during MILDEX. Journal of physical oceanography, 17(4), 425-439.

[8] Buranathanitt, T., 1979. Some effects of Langmuir circulation on suspended particles in lakes and reservoirs. Ph.D. Thesis, Leicester University Engineering Department, England, Chapter1.

[9] Stewart, R. H. (2008). Introduction to physical oceanography (pp. 133-147). College Station:Texas A & M University.

[10] Gargett, A.E., J.R. Wells, A.E. Tejada-Martinez and C.E. Grosch (2004) "Langmuir supercells: A dominant mechanism for sediment resuspension and transport", Science, 306, 1925-1928.

[11] Dethleff, Dirk, and E. W. Kempema. "Langmuir Circulation Driving Sediment Entrainment into Newly Formed Ice: Tank Experiment Results with Application to Nature (Lake Hattie, United States; Kara Sea, Siberia)." Journal of Geophysical Research 112, no. C2 (2007). doi:10.1029/2005jc003259.

[12] Chiba, David, and Burkard Baschek. "Effect of Langmuir Cells on Bubble Dissolution and Air-sea Gas Exchange." Journal of Geophysical Research 115, no. C10 (2010). doi:10.1029/2010jc006203.